Role of Second Coordination Sphere Amino Acid Residues on the Proton Transfer Mechanism of Human Carbonic Anhydrase II (HCA II)

ARTICLE *in* THE JOURNAL OF PHYSICAL CHEMISTRY A · AUGUST 2010

Impact Factor: 2.69 · DOI: 10.1021/jp101515h · Source: PubMed

2 AUTHORS, INCLUDING:

Hakkim Vovusha

King Abdullah University of Science and Te…

12 PUBLICATIONS **51** CITATIONS

SEE PROFILE

Role of Second Coordination Sphere Amino Acid Residues on the Proton Transfer Mechanism of Human Carbonic Anhydrase II (HCA II)

V. Hakkim and V. Subramanian*

Chemical Laboratory, Central Leather Research Institute, Council of Scientific and Industrial Research, Adyar, Chennai 600 020, India

Received: February 19, 2010; Revised Manuscript Received: June 7, 2010

The barrier for the proton transfer in human carbonic anhydrase II (HCA II) has been studied by including the important second coordination sphere residues to the minimalistic model of the active site using B3LYP/6-31+G** level of calculation. Specifically, proton transfer from a zinc-bound water molecule to a histidine residue (His64) mediated by a water bridge (consists of two and three water molecules) has been investigated. The new model contains three functional groups of second coordination sphere residues such as Gln92, Glu117, and Asn244. These residues interact with His94, His119, and His96, respectively. We have calculated the barrier for the proton transfer using the total energies of reactants, transition states, and products. The calculated barrier height for the models with two water and three water molecules are 8.94 and 8.67 kcal/mol, respectively, which are in close agreement with the experimental value of 7.8 kcal/mol obtained from the kinetic experiments and to the range 8−10 kcal/mol predicted from the pK_a considerations (Silverman, D. N. *Biochim. Biophys. Acta* **2000**, *1458*, 88−103.). In addition, our own N-layered integrated molecular orbital + molecular mechanics (ONIOM) calculations have also been carried out on various model systems to understand the effect of complete environment. It is possible to note from the results that the confinement of water molecules by the protein milieu appreciably decreases the O···O distance between water molecules in the water bridge when compared to the free water dimer which enables the proton transfer from one water to the other and finally to the His64 residue.

Introduction

Carbonic anhydrase (CA) was discovered more than 70 years ago. It contains zinc as a cofactor for its catalytic activity. CA catalyzes the reversible hydration of the carbon dioxide. It is an important reaction that is implicated in many physiological processes such as respiration, photosynthesis or acid−base balance of all living organisms.[1,2] All CAs are zinc metalloenzymes. In addition, some CAs are monomers (α) while others are tetramers (*β*, *γ*), hexamers (*β*), or octamers (*β*) and all isoenzymes are single-chain polypeptides with the molecular weight of 30 kDA and contain one zinc ion per molecule. The shape of this enzyme is similar to the rugby ball with a crevice 16 Å deep running through the south pole.[2] At the bottom of the crevice, the zinc ion is anchored to the protein by three histidine nitrogen atoms and is exposed to water. Two histidine residues, His94 and His96, are coordinated to zinc by means of their Nε2 atoms. The third histidine residue, His119 is bound to zinc through its Nδ1 atom. Depending on the pH, one or two water molecules are coordinated to zinc.[3] At low pH, the coordination number of the zinc is four and it contains one water molecule. It is found from the X-ray crystallographic studies that intricate hydrogen bonding network exists around the zinc site.[4−7] The three histidine NH protons are hydrogen bonded with other residues in the enzyme. The His119 is hydrogen bonded to the Glu117. The side chain of Gln92 and the peptide linkage of Asn244 is hydrogen bonded to the second nitrogen of imidazole moiety of His94 and His96, respectively. The coordinated water molecule is hydrogen bonded to Thr199 which in turn hydrogen bonded to Glu106.[8,9]

Numerous experimental and computational studies have been carried out on the structure−function relationship of HCA II.[10−16] Silverman and co-workers have made several significant contributions to the understanding of proton transfer mechanism of HCA II.[17−20] Voth and co-workers have used molecular dynamics (MD) and quantum mechanical/molecular mechanical (QM/MM) simulation to understand the proton transfer mechanism.[21−23] Especially multiscale empirical valence bond (MS-EVB) method accurately models the proton transfer reaction in the solution and also it reproduces the experimental proton transfer values of the HCA II. These studies have unveiled that the catalytic reaction proceeds in two steps.[7,24] The first stage of the reaction involves the reaction of CO_2 with the zinc-bound hydroxyl ion to form the product HCO_3^-, then dissociation of HCO_3^- takes place from the active site, and the vacant coordination site of the zinc ion is occupied by a water molecule as shown in Figure 1. In the second stage, a proton transfers from the zinc-bound water molecule to the bulk through a histidine residue (His64) as shown in Figure 2. This process regenerates the active species, that is, the zinc-bound hydroxyl ion. In this context, it is noteworthy to mention about the seminal work of Cui and Karplus on the energetics of proton transfer reactions in CA using the minimalistic model for the active site.[25] The proton transfer from the zinc-bound water molecule to His64 residue mediated by several water molecules was investigated. It was demonstrated that the proton transfer reaction in CA is sensitive to the nature and structure of the water bridge, which would be influenced by the dynamics of the water molecules and amino acids in the active site of the protein. Furthermore, as the number of water molecules in the bridge increases from two to four, the proton transfer changes

* To whom correspondence should be addressed. Fax: +91-44-24411630. E-mail: subuchem@hotmail.com, subbu@clri.res.in.

10.1021/jp101515h
Published on Web 07/13/2010

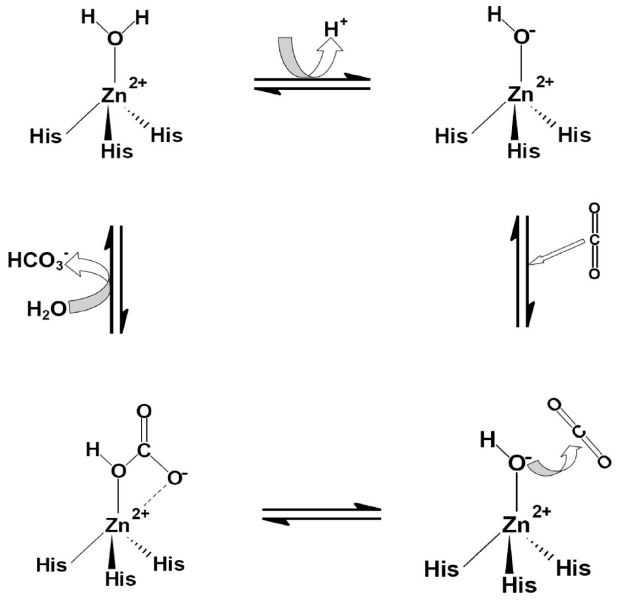

Figure 1. Schematic representation of catalytic mechanism of HCA II using the minimalistic active site model.

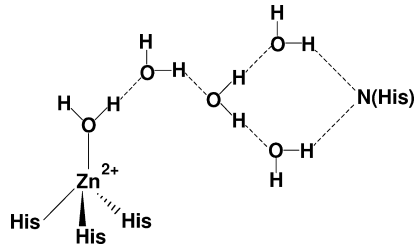

Figure 2. Schematic representation of proton transfer mechanism in HCA II.

from being fully concerted (W_2), through partially concerted (W_3) to stepwise (W_4).[25] It is clear from this study that the active site model is not sufficient and the inclusion of protein environment is necessary to gain further insight into the proton transfer process.

The role of second coordination sphere residues and its influence on the structure and functions of HCA II have been explained.[26,27] Lin et al have reported a systematic theoretical study on the factors governing the His protonation/deprotonation state in Zn-binding sites.[28] Various issues addressed in that study are (i) the role of composition of first coordination sphere ligands and solvent accessibility on the transfer of the Zn-bound His imidazole proton to the second coordination sphere Asp/Glu carboxylate oxygen, (ii) the proton accepting nature of any second coordination sphere ligand such as backbone carbonyl oxygen, and (iii) the importance of Asp/Glu in the Zn-His-Asp/Glu triad on the protonation state of a Zn-bound water. Particularly, this triad plays structural and electronic roles in orienting the first coordination ligands, fine-tuning the pK_a and the reactivity of zinc bound water molecule.[28−30] Recently, Frison et al. have probed the role of Zn-His-Glu triad by considering various models consist of 37−101 atoms.[31] They have shown that the carboxylate group of the Glu117 acts as a hydrogen bond acceptor in the hydroxyl form of HCA II, whereas the same ligand behaves as either a hydrogen bond acceptor or donor in the aqua form of HCA II. Therefore the chemistry of a zinc-bound water molecule is altered by the second shell ligands.

In the prediction of enzyme reaction mechanism, several model studies have been made by employing minimalistic and

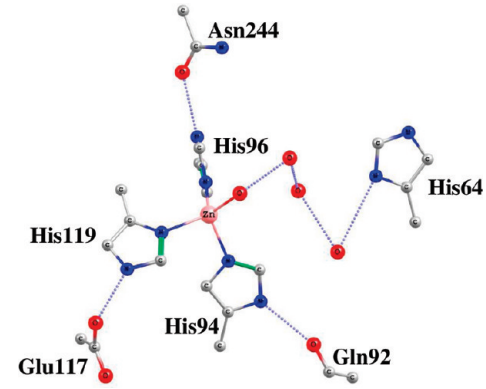

Figure 3. Active site model of HCA II with second shell amino acids.

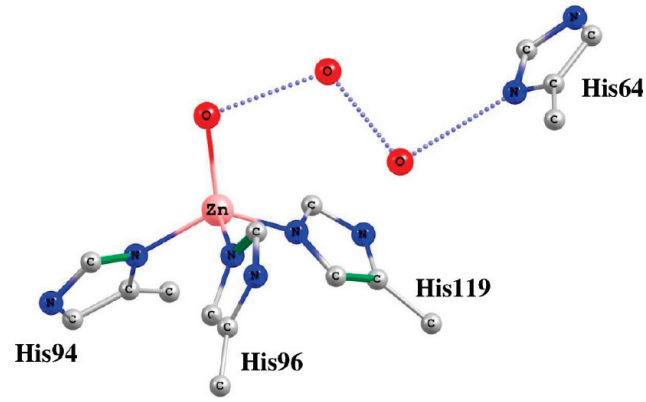

Figure 4. Active site of Model-1.

cluster models.[11,32−34] With the advancement in the hardware and computational methodologies, it is now possible to include the full protein structure using QM/MM and our own N-layered integrated molecular orbital + molecular mechanics ONIOM methodologies.[35] The usefulness and success of QM/MM and ONIOM approaches in the prediction of enzyme reaction mechanism and spectral properties have been documented.[36−38]

In the present study, the effect of second shell ligands (Gln92, Glu117, and Asn244) on the proton transfer mechanism of HCA II has been investigated using density functional theory (DFT)-based Becke's three parameter exchange correlation and Lee−Yang−Parr correlation functional (B3LYP) method employing the 6-31+G** basis set.[39−43] Since, the proton transfer from a zinc-bound water molecule to His64 residue is mediated by several molecules, the proton transfer through water bridges consisting of two and three water molecules has been modeled by calculating the geometries and energies of all the reactants, products, transition states, and intermediates using concerted mechanism. Although our model may not incorporate the entire important environment, some of the important second coordination sphere amino acids that interact with the metal coordinating ligands are included.

Computational Details

Figure 3 describes the active site model of HCA II built from the X-ray crystallographic structure (PDB code 2CBA, 1.54 Å resolution). The minimalistic model for the HCA II is designated as Model-1 in the remaining part of the text. It can be seen from Figure 4 that Model-1 consists of the zinc ion, the side chains of three histidine residues, (His94, His96, and His119), the coordinated water molecule, the water bridge made up of two water molecules, and the proton accepting residue, His64.

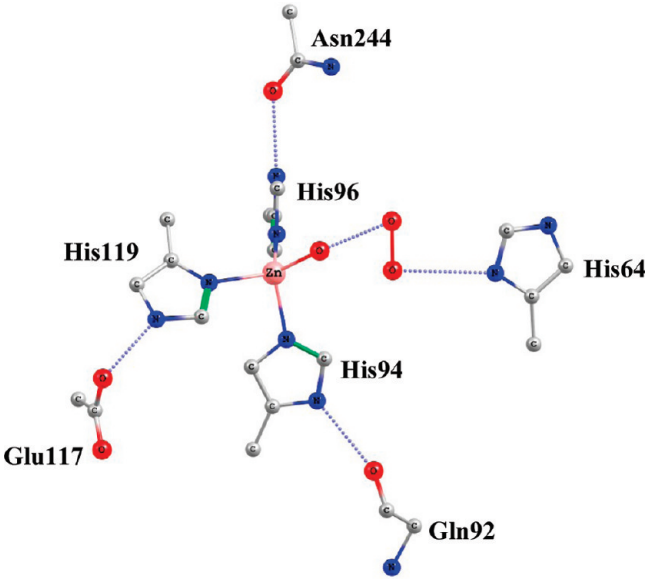

Figure 5. Active site of Model-2.

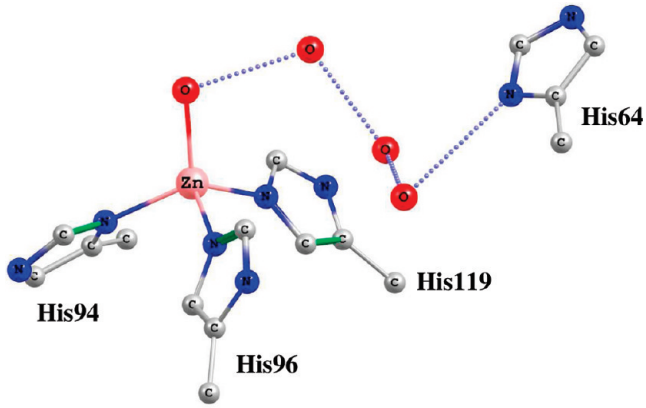

Figure 6. Active site of Model-3.

The Model-2 is composed of Model-1 with important second coordination sphere residues and it is illustrated in Figure 5. The Model-1 with an additional water molecule is designated as Model-3. The same model with second coordination sphere ligands is referred to as Model-4. Both Model-3 and Model-4 are shown in Figure 6 and 7, respectively.

The initial coordinates of the non-hydrogen atoms were taken from the X-ray structure of HCA II.[44] Hydrogen atoms were added using Gauss view package.[45] Since, the "inward" conformer of His64 was observed in the X-ray structure, the same arrangement was chosen for the present study. To mimic the protein environment in the crystal structure, the positions of the Cβ atoms were fixed during the geometry optimization. Remaining atoms were optimized without any constraints. The B3LYP method has shown to be a promising tool in exploring the reaction mechanism of transition metal containing enzymes.[46] Thus the geometries of all the stable structures and saddle points were fully optimized at the B3LYP/6-31+G** level. A single imaginary frequency criterion was used for the characterization of transitions states. The reaction energies were corrected to zero-point energy (ZPE). Natural bond orbital (NBO) analysis was used to calculate atomic charges of all the models. All calculations were performed using Gaussian 03 package.[47]

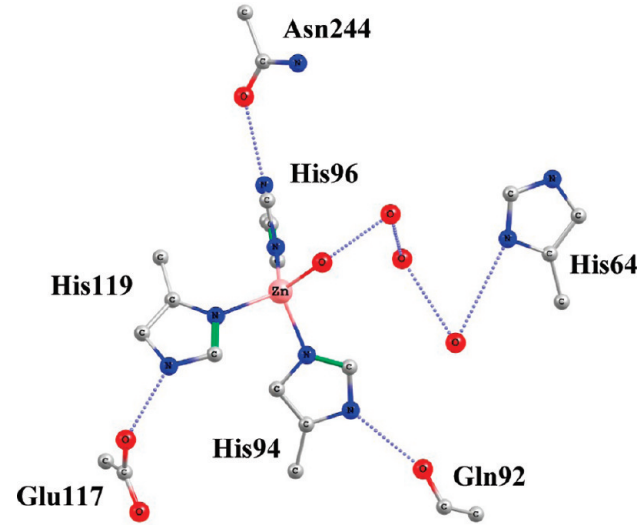

Figure 7. Active site of Model-4.

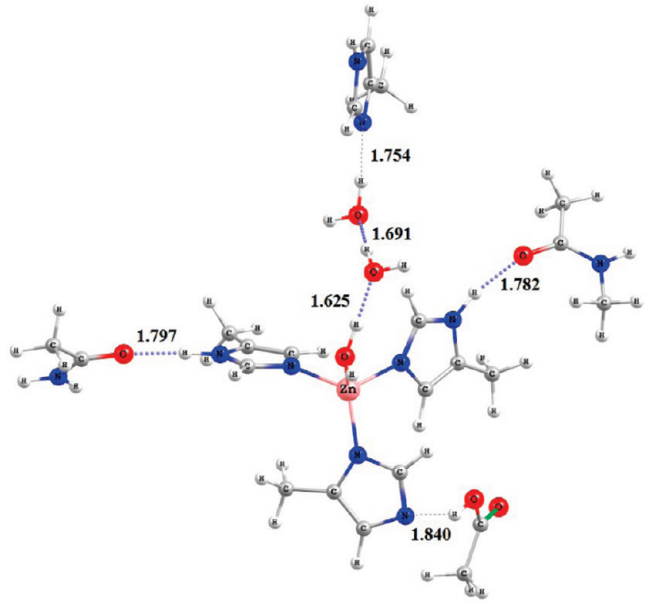

Figure 8. Optimized geometry of Model-2 at B3LYP/6-31+G** level of calculation.

ONIOM Calculation

To elucidate the role of protein environment on the PT transfer reaction of HCA II, two-layer ONIOM calculations were performed. In two water model, out of total number of 4081 atoms, 54 atoms were treated at high level (B3LYP/6-31+G**) and 4027 atoms were treated at low level using universal force field (UFF). In the three water systems, 57 and 4027 atoms were treated at high and low levels, respectively. Although, the geometries of the reactants and products were successfully optimized using ONIOM method, we could not locate the transition states for the proton transfer reactions.

Results and Discussion

Geometries of the Model Systems with Second Coordination Sphere Amino Acid Residues. The optimized geometries of reactants of Model-2 and Model-4 are shown in Figure 8 and 9, respectively. The geometrical parameters and NBO charges of all the models are shown in Table 1. It can be seen from the geometrical parameters that Zn−O distance of Model-2

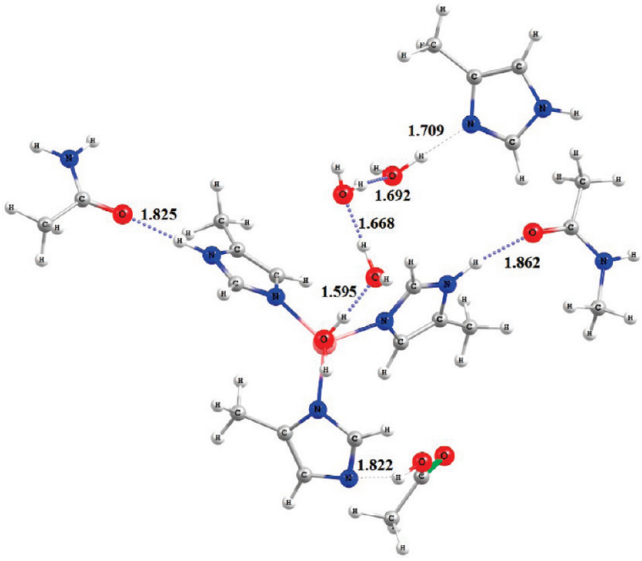

Figure 9. Optimized geometry of Model-4 B3LYP/6-31+G** level of calculation.

TABLE 1: Geometrical Parameter and NBO Charges of the Model Systems

	Bond Distance (Å)			
	Model-1	Model-2	Model-3	Model-4
Zn−O	2.044	2.077	2.037	2.067
	NBO charges			
	Model-1	Model-2	Model-3	Model-4
Zn	1.285	1.266	1.284	1.269

and Model-4 are larger than the corresponding Model-1 and Model-3. Since, the charge on the Zn decreases in the presence of second-shell ligands, the coordinated water molecule is less bound to the metal atom when compared to Model-1. Besides, after the optimization the NH-proton of His119 moves toward Glu117 and thus it acts as a proton acceptor. This observation is similar to that found in a previous study.[29] In that study, two isomers, one containing a Zn^{2+}-$ImH^0\cdots MeCOO^-$ (NH isomer) and the other Zn^{2+}-$Im^-\cdots MeCOOH^0$ (OH isomer) units were investigated. It was found that due to the high Lewis acidity of Zn, the $Im^-\cdots MeCOOH$ moiety is more stable than the $ImH^0\cdots MeCOO^-$, and consequently the OH isomer is lower in energy than the NH isomer. Our results reinforce these findings.

Two Bridging Waters. The calculations on Model-1 and Model-2 reveal that only one transition state exists for the proton transfer reaction from the Zn-bound water molecule to the His64. The optimized geometries of the reactants, transition states, and products corresponding to Model-1 and Model-2 are shown in Figures 10 and 11, respectively. In the transition state of Model-1, the proton-donor distances are 1.105, 1.148, and 1.359 Å, and the corresponding proton-acceptor distances are 1.332, 1.280, and 1.172 Å, respectively. These distances show that first two protons are near to the donor atoms and the third proton is closer to the acceptor atom. Although existence of Eigen cation in the transition state has been observed in the previous study,[25] we could not detect the same from the donor-proton and proton-acceptor distances. The donor-proton (acceptor-proton) distances in the transition state corresponding to Model-2 are 1.172 (1.250), 1.344 (1.105), and 1.387 (1.40) Å. The geometrical parameters observed from the transition state corresponding to Model-2 indicate that the presence of second coordination ligands has marginal influence on the proton-donor and proton-acceptor distances in the water chain. Comparison of various geometrical parameters of the two models reveal that the hydrogen-bonding interaction of second coordination sphere amino acid residues with metal coordinated histidines leads to appreciable changes in the primary coordination environment. Consequently, Zn−O distance increases by 0.03 Å in the case of Model-2 when compared to Model-1 (Table 1).

The calculated barrier for the concerted proton transfer for Model-1 at the B3LYP/6-31+G** level of theory is 5.0 kcal/mol. However, the inclusion of ZPE correction decreases the barrier to 0.44 kcal/mol. The same proton transfer barrier for Model-2 with second coordination sphere residues is 13.69 kcal/mol. The inclusion of with ZPE correction reduces to 8.94 kcal/mol.

Three Bridging Waters. The calculated geometries of the reactants, the transition states, and the products for Model-3 and Model-4 are shown in Figures 12 and 13, respectively. In this model, the proton transfer involves four protons. It is found from the calculation that only one transition state exists in the transfer of proton from the water molecule coordinated to the zinc to the His64. Close scrutiny of the geometrical parameters of transition state reveals that the donor-proton distances in Model-3 are 1.101, 1.103, 1.382, and 1.578 Å, and for the same model corresponding proton-acceptor distances are 1.334, 1.341, 1.088, and 1.076 Å, respectively. It can be seen from the various donor and acceptor distances that the proton is about to be transferred to the His64. The calculated barrier for the proton transfer without ZPE is 6.15 kcal/mol. Upon inclusion of the same it becomes 2.8 kcal/mol.

The donor-proton (acceptor-proton) distances in the transition state for Model-4 are 1.080 (1.388), 1.199 (1.213), 1.307 (1.120), and 1.362 (1.150) Å. The calculated barrier is 13.97 kcal/mol (without ZPE). Upon inclusion of ZPE correction, it turns out to be 8.67 kcal/mol. Comparison of results shows that the barrier for proton transfer involving three water molecules is higher than that through two water molecules.

Energetic of Proton Transfer Reaction. The energetics of the proton transfer reactions without and with ZPE for various models of HCA II is shown in Figures 14 and 15, respectively. Apparently, the barrier for proton transfer increases with the increase in the number of water molecules. The barrier height for the proton transfer is 5.00 and 6.15 kcal/mol for Model-1 and Model-3, respectively. These values are lower than that estimated from kinetic measurements (7.8 kcal/mol) or pK_a considerations (8−10 kcal/mol).[1] Corresponding exothermicities of the two models are 5.3 and 6.9 kcal/mol. The inclusion of second shell amino acids increases the barrier for the proton transfer. The calculated values for Model-2 and Model-4 are 13.69 and 13.97 kcal/mol, respectively. Furthermore, the inclusion of the second shell ligands changes the reaction to endothermic and the endothermicity of Model-2 and Model-4 are 12.55 and 9.03 kcal/mol, respectively.

The ZPE-corrected barrier heights for Model-1 and Model-3 are 0.44 and 2.81 kcal/mol, respectively. The same for Model-2 and Model-4 are 8.94 and 8.67 kcal/mol, respectively. It can be seen that the proton transfer barrier for Model-1 and Model-3 is considerably lower than that of experimental values. A similar trend has also been observed in the previous study.[25] It is found that B3LYP/6-311+G**//B3LYP/6-31G* method yields a value of 5.9 kcal/mol for the proton transfer barrier for the active site model in which proton transfer is mediated by two water molecules. After incorporation of ZPE correction, it decreases

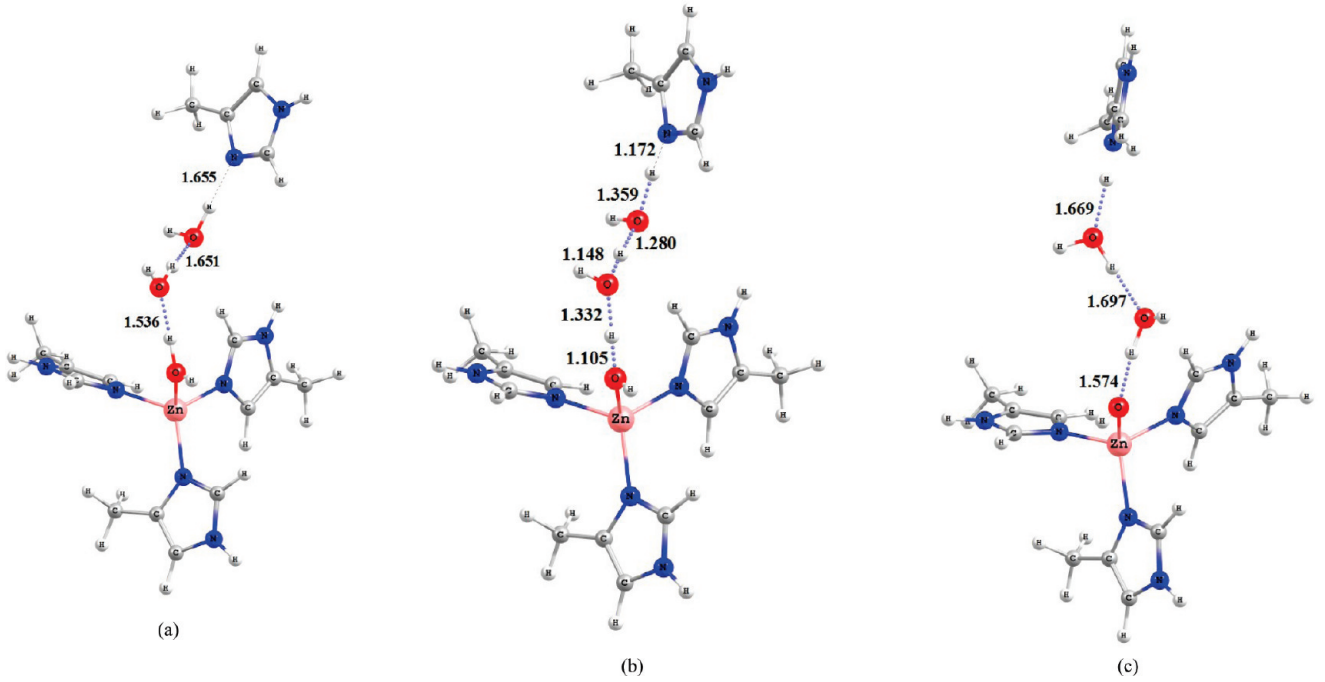

Figure 10. Optimized structures of Model-1 [(a) reactant, (b) transition state, (c) product] at B3LYP/6-31+G** level of calculation.

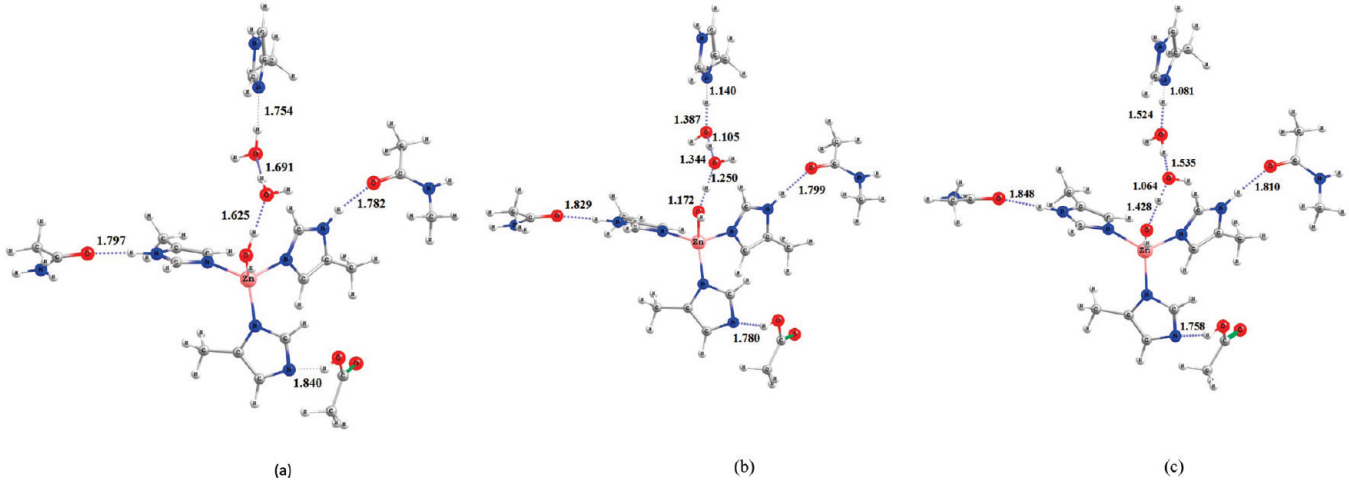

Figure 11. Optimized structures of Model-2 [(a) reactant, (b) transition state, (c) product] at B3LYP/6-31+G** level of calculation.

to 0.6 kcal/mol. The same study predicted a value of 8.6 kcal/mol for the proton transfer mediated by the three water molecules without ZPE. After ZPE corrections, it turns out to be 3.6 kcal/mol.[25] Both models could not correctly predict the experimental value due to the absence of second coordination ligands. It is possible to note from the present study that the inclusion of second coordination sphere ligands in the calculation reasonably yields reliable estimates of proton transfer barrier. The ZPE-corrected proton transfer barrier for Model-2 (8.94 kcal/mol) and Model-4 (8.67 kcal/mol) is closer to the experimental value than the previously reported values.[1] The trends obtained from the present calculation reveals that the inclusion of full protein environment will significantly influence the barrier for the proton transfer. However, the interplay of other amino acid residues that are hydrogen bonded to the second coordination sphere ligands needs to be explored.

It can be seen from Figure 15 that the relative energy of the product for Model-2 and Model-4 is higher than that of corresponding transition state. This may be because the proton from the zinc bound water molecule is not completely transferred. To rule out the possibility that it may be an intermediate, we have performed geometry optimization on the products with proton completely transferred condition. The calculations yield similar structures indicating that the product of Model-2 and Model-4 is true minima on the potential energy surface and the absences of imaginary frequencies reinforce the same findings. From these studies, the experimental value of barrier for the proton transfer reaction is achieved by including second shell ligands. However, it switches the reaction from exothermic to endothermic. In realistic situation, the interaction of second shell ligands with other residues may change the endothermicity of the reaction.

It is well-known that CA is an enzyme in which reasonably long-range proton transfer over a distance of ~8 Å) is shown to play an important role. Therefore the distance between the proton donor (Zn) and acceptor (N) of His64 appears to be significant factor for the efficiency of proton transfer in HCA II.[48,49] The donor−acceptor distances for various models are presented in Table 2. The calculated values are in close agreement with that for the wild type of enzyme, which implies

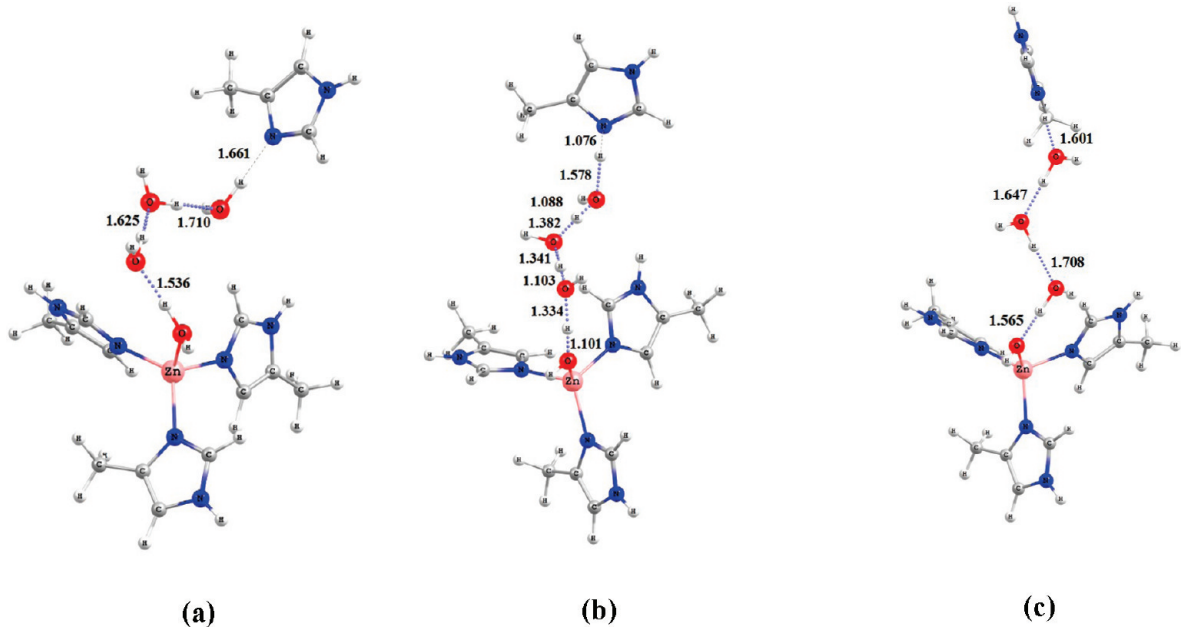

Figure 12. Optimized structures of Model-3 [(a) reactant, (b) transition state, (c) product] at B3LYP/6-31+G** level of calculation.

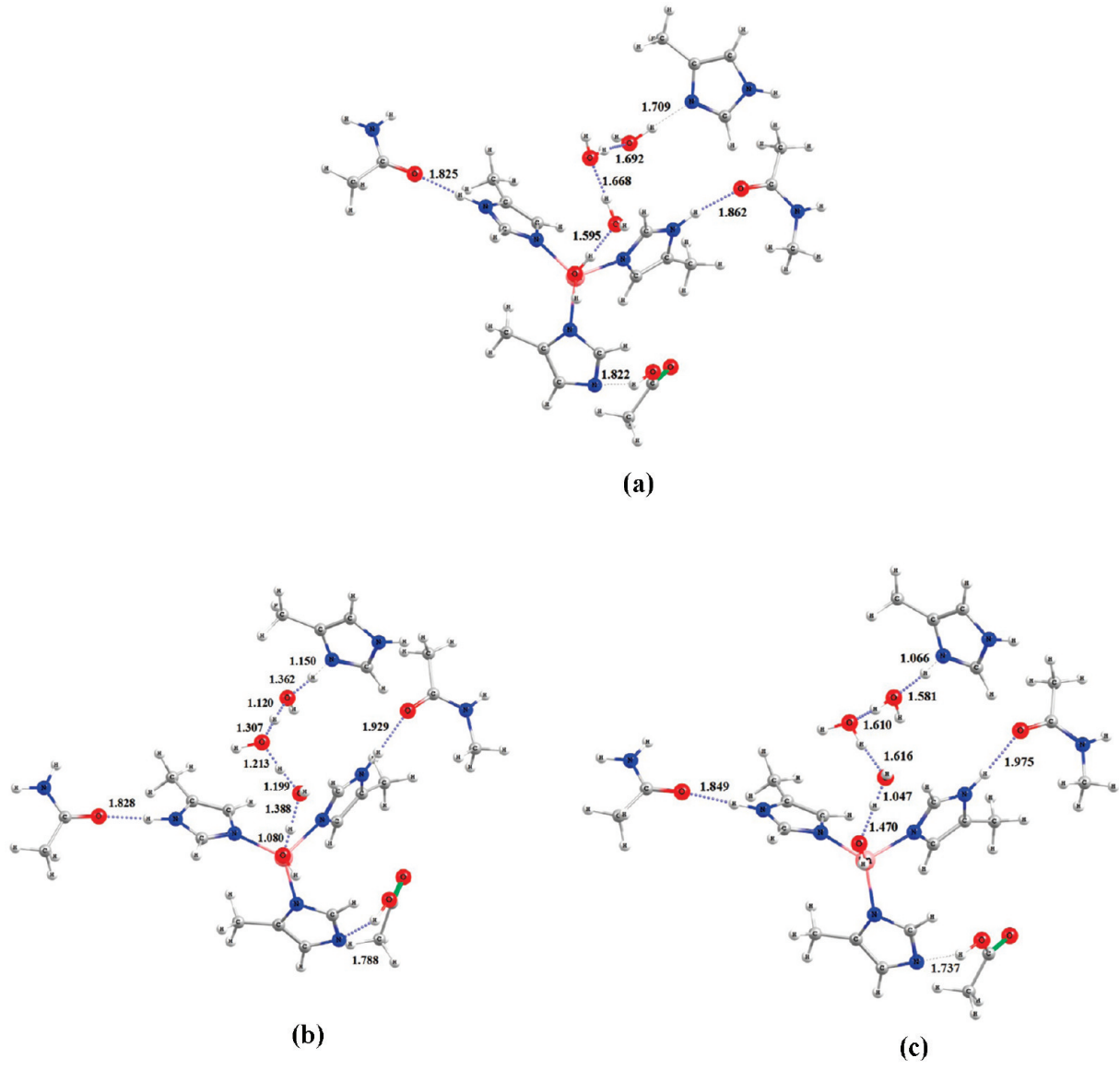

Figure 13. Optimized structures of Model-4 [(a) reactant, (b) transition state, (c) product] at B3LYP/6-31+G** level of calculation.

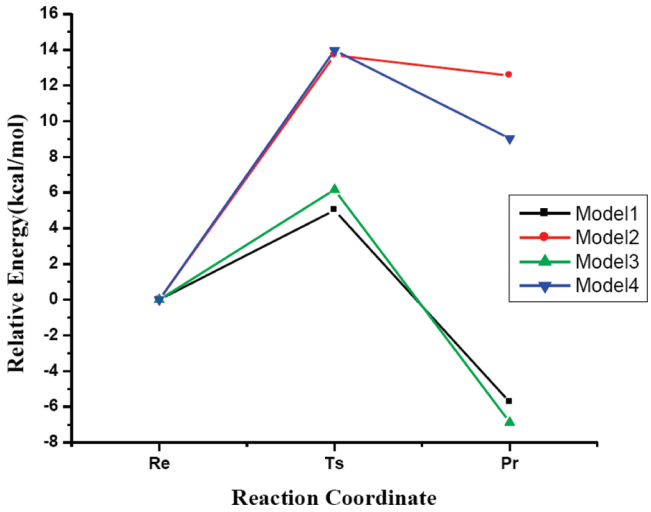

Figure 14. Comparison of potential energy profiles for the various models (without ZPE).

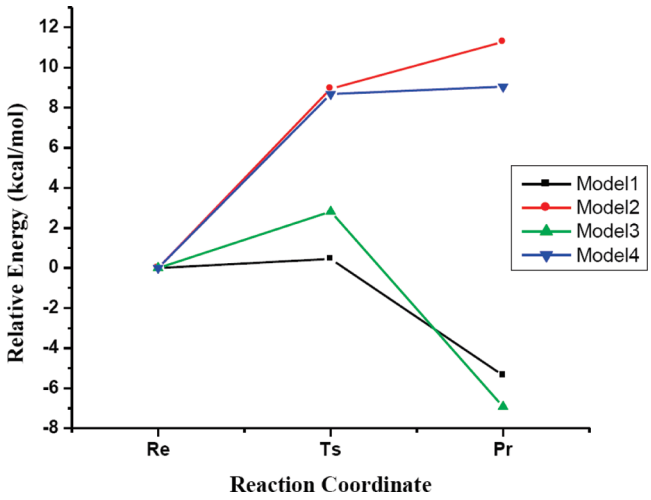

Figure 15. Comparison of potential energy profiles for the various models (with ZPE).

TABLE 2: Donor−Acceptor Distances in Various Models

models	donor(zn)−acceptor(N-His64) (Å)
Model-1	7.6
Model-2	7.8
Model-3	7.7
Model-4	7.5
wild type	7.5

that the selected models are sufficiently reliable to predict the proton transfer reaction.

ONIOM Calculation of Proton Transfer Reaction of HCAII. Optimized geometries of reactants and products are presented in the Supporting Information (Figures S1−S4). Since the initial geometries of the transition states adopted during optimization, we could not explain the effect of protein environment on the geometries of transition states and energetics of proton transfer reaction. However, the calculated geometrical parameters of the reactants and products in the presence of full protein environment yield valuable clues. The donor-proton (acceptor-proton) distances in the reactant of the two water model are 1.019 (1.544), 1.0 (1.679), and 1.023(1.661) Å. The same distances in the product are 1.544 (1.022), 1.603 (1.011), and 1.644 (1.056) Å. In the case of the three water model, the donor-proton (acceptor-proton) distances in the reactant are 1.034 (1.473), 1.004 (1.599), 1.007 (1.615), and 1.020 (1.650) Å. The similar distances in the product are 1.553 (1.016), 1.559 (1.009), 1.630 (1.002), and 1.582 (1.062) Å. The comparison of the geometrical parameters obtained from the ONIOM calculation with the models show that the donor-proton (acceptor-proton) distances are influenced by the presence of protein environment.

TABLE 3: O···O Distances between Two Water Molecules in the Bridge for Various Models

D_{O-O} (Å)	Model-1	Model-3	Model-2	Model-4
reactant	2.64	2.68	2.62	2.65
			2.70	2.67
transition state	2.42	2.44	2.44	2.41
			2.46	2.42
product	2.69	2.55	2.70	2.61
			2.64	2.60
water dimer	2.88[a]			

[a] (B3LYP/6-31+G**).

Relative Importance of Asn and Gln Compared to the Glu. To quantify the relative importance of Asn and Gln residues on the proton transfer reaction, the calculations were performed without these residues. The geometries of reactants, transition states, and products were optimized at the B3LYP/6-31+G** level of theory. Optimized geometry of reactant, transition state, and product for the two (Model-5) and three water (Model-6) are given in the Supporting Information (Figures S5 and S6). The calculated barrier for the proton transfer barrier without Asn and Gln residues for two water model is 12.18 kcal/mol. The same for the three water model is 13.43 kcal/mol. The comparison of these values with that in the presence of Glu117 (current models) reveals that these residues play a marginal role in the modulation of proton transfer reaction. To assess the significance of Glu117, the calculations were performed without Glu117 to assess its importance. Optimized geometry of reactant, transition state, and product for the two (Model-7) and three water (Model-8) are given in the Supporting Information (Figures S7 and S8). The calculated barrier for the two water (Model-7) and three water (Model-8) models are 6.48 and 11.99 kcal/mol, respectively. The evidence elicits that Glu117 plays an important role when compared to the Asn and Gln residues. The changes in the second coordination ligands influence the charge on the metal ion and thereby modulate the proton transfer reaction. The calculated charges on the Zn atom in different model are shown in Table 1 in the Supporting Information.

Effect of Tyr7 on the PT Reaction of HCA II. Recently Fisher et al. have reported the structure (at pH 9.0) obtained from the neutron diffraction studies.[18] It is found that Tyr7 is observed in the unprotonated form. However, there are no clear details about the role of Tyr7 in the PT reaction. Hence, an attempt was made to assess the role of Tyr7 in the PT process. The calculations were performed on various model systems to understand the part played by the unprotonated form of Tyr7. The optimized geometries of model systems are depicted in the Supporting Information (Figure S9 and S10). The results reveal that due to strong proton accepting power, the proton is transferred to Tyr7 without any energy barrier.

Structural Reorganization of Water Molecules. The calculated O···O distances of water molecules present in the bridge connecting the donor (active site), acceptor (His64), and free water dimer are presented in Table 3. It can be observed that the water molecules undergo significant structural confinement due to the protein environment. The O···O distance (D_{O-O})

between any two consecutive water molecules in the bridge of the reactants and products is considerably less than that of the free water dimer. Furthermore, D_{O-O} still decreases in the transition state, which facilitates the proton transfer from one water molecule to other.

Conclusion

In this investigation, the energy barrier for the proton transfer reaction in HCA II has been calculated by considering different models for the active site and water bridge. The barrier for the proton transfer increases with increase in the number of water molecules in the bridge. This observation clearly shows that solvent environment significantly influences the barrier for the proton transfer. ZPE corrected barrier for the proton transfer reaction for Model-2 and Model-4 is 8.94 and 8.67 kcal/mol, respectively, which is in good agreement with the experimental value.[1] Furthermore, it is found that the presence of second coordination sphere significantly influences the proton transfer reaction. In addition, the confinement of water molecules by the protein environment significantly decreases the O···O distance between any water molecules in the water bridge when compared to the free water dimer, which facilitates the proton transfer from one water to the other and finally to the His64.

Acknowledgment. This study is supported by the grant from the Department of Science and Technology (DST), Government of India, New Delhi, India, under New Initiatives in Bioinorganic Chemistry. The authors wish to thank Dr. T. Ramasami for his valuable suggestions and comments and Dr. A. B. Mandal, Director, CLRI for his continued support.

Supporting Information Available: Additional table and figures. This material is available free of charge via the Internet at http://pubs.acs.org.

References and Notes

(1) Silverman, D. N. *Biochim. Biophys. Acta* **2000**, *1458*, 88–103.
(2) Messerschmidt, A.; Huber, R.; Poulos, T.; Wieghardt, K. *Metalloproteins*; John Wiley and Sons: New York, 2001; Vols. *I*, II.
(3) Bertini, I.; Gray, H. B.; Lippard, S. J.; Valentine, J. S. *Bioinorganic Chemistry*; University Science Books: Sausalito, CA, 2007.
(4) Silverman, D. N.; Mckenna, R. *Acc. Chem. Res.* **2007**, *40*, 669–675.
(5) Eriksson, A. E.; Jones, A. T.; Liljas, A. *Proteins* **1988**, *4*, 274–282.
(6) Cox, J. D.; Hunt, J. A.; Compher, K. M.; Fierke, C. A.; Christianson, D. W. *Biochemistry* **2000**, *39*, 13687–13694.
(7) Lindskog, S. *Pharmacol. Ther.* **1997**, *74*, l–20.
(8) Christianson, D. W.; Fierke, C. A. *Acc. Chem. Res.* **1996**, *29*, 331–339.
(9) Christianson, D. W.; Cox, J. D. *Annu. Rev. Biochem.* **1999**, *68*, 33–57.
(10) Krishnamurthy, V. M.; Kaufman, G. K.; Urbach, A. R.; Gitlin, I.; Gudiksen, K. L.; Weibel, D. B.; Whitesides, G. M. *Chem. Rev.* **2008**, *108* (3), 946–1051.
(11) Bottoni, A.; Lanza, C. Z.; Miscione, G. P.; Spinelli, D. *J. Am. Chem. Soc.* **2004**, *126* (5), 1542–1550.
(12) Lipton, A. S.; Heck, R. W.; Ellis, P. D. *J. Am. Chem. Soc.* **2004**, *126* (14), 4735–4739.
(13) Marino, T.; Russo, N.; Toscano, M. *J. Am. Chem. Soc.* **2005**, *127* (12), 4242–4253.
(14) Roy, A.; Taraphder, S. *J. Phys. Chem. B* **2007**, *111*, 10563–10576.
(15) Roy, A.; Taraphder, S. *J. Chem. Sci.* **2007**, *119*, 545–552.
(16) Röthlisberger, U. *ACS Symp. Ser.* **1998**, *712*, 264–274.
(17) Fisher, S. Z.; Tu, C.; Bhatt, D.; Govindasamy, L.; Agbandje-McKenna, M.; McKenna, R.; Silverman, D. N. *Biochemistry* **2007**, *46*, 3803–3813.
(18) Fisher, S. Z.; Kovalevsky, A. Y.; Domsic, J. F.; Mustyakimov, M.; McKenna, R.; Silverman, D. N.; Langan, P. A. *Biochemistry* **2010**, *49* (3), 415–421.
(19) Avvaru, B. S.; Kim, C. U.; Sippel, K. H.; Gruner, S. M.; Agbandje-McKenna, M.; Silverman, D. N.; McKenna, R. *Biochemistry* **2010**, *49* (2), 249–251.
(20) Zheng, J.; Avvaru, B. S.; Tu, C.; McKenna, R.; Silverman, D. N. *Biochemistry* **2008**, *47* (46), 12028–12036.
(21) Maupin, C. M.; Zheng, J.; Tu, C.; McKenna, R.; Silverman, D. N.; Voth, G. A. *Biochemistry* **2009**, *48* (33), 7996–8005.
(22) Maupin, C. M.; McKenna, R.; Silverman, D. N.; Voth, G. A. *J. Am. Chem. Soc.* **2009**, *131* (22), 7598–7608.
(23) Maupin, C. M.; Saunders, M. G.; Thorpe, I. F.; McKenna, R.; Silverman, D. N.; Voth, G. A. *J. Am. Chem. Soc.* **2008**, *130* (34), 11399–11408.
(24) Chegwidden, W. R.; Carter, N. *The Carbonic Anhydrases: New Horizons*; Chegwidden, W. R.; Carter, N. D., Edward, Y. H., Eds.; Birkhäuser Verlag: Basel, Switzerland, 2000.
(25) (a) Cui, Q.; Karplus, K. *J. Phys. Chem. B* **2003**, *107*, 1071–1078.
(26) Maret, W.; Li, Y. *Chem. Rev.* **2009**, *109* (10), 4682–4707.
(27) Auld, D. S. *Biometals* **2009**, *22*, 141–148.
(28) Lin, Y. L.; Lim, C. *J. Am. Chem. Soc.* **2004**, *126*, 2602–2612.
(29) Nakagawa, S.; Umeyama, H.; Kitaura, K.; Morokuma, K. *Chem. Pharm. Bull. (Tokyo)* **1981**, *29*, 1.
(30) El Yazal, J.; Roe, R. R.; Pang, Y. P. *J. Phys. Chem. B* **2000**, *104*, 6662.
(31) Frison, G.; Ohanessian, G. *Phys. Chem. Chem. Phys.* **2009**, *11*, 374–383.
(32) Siegbahn, P. E. M.; Himo, F. *J. Biol. Inorg. Chem.* **2009**, *14*, 643–651.
(33) Siegbahn, P. E. M. *J. Am. Chem. Soc.* **2009**, *131*, 18238–18239.
(34) Siegbahn, P. E. M. *Inorg. Chem.* **2008**, *47*, 1779–1786.
(35) Metz, S.; Thiel, W. *J. Phys. Chem. B* **2010**, *114*, 1506–1517.
(36) Shaik, S.; Cohen, S.; Wang, Y.; Chen, H.; Kumar, D.; Thiel, W. *Chem. Rev.* **2010**, *110*, 949–1017.
(37) Senn, H. M.; Thiel, W. *Angew. Chem., Int. Ed.* **2009**, *48*, 1198–1229.
(38) Rajapandian, V.; Hakkim, V.; Subramanian, V. *J. Phys. Chem. A* **2009**, *113*, 8615–8625.
(39) Lee, C.; Yang, W.; Parr, R. G. *Phys. Rev. B* **1988**, *37*, 785.
(40) Becke, A. D. *Phys. Rev. A* **1988**, *38*, 3098–3100.
(41) Becke, A. D. *J. Chem. Phys.* **1992**, *96*, 2155–2160.
(42) Becke, A. D. *J. Chem. Phys.* **1992**, *97*, 9173–9177.
(43) Becke, A. D. *J. Chem. Phys.* **1993**, *98*, 5648–5652.
(44) Hakansson, K.; Carlsson, M.; Svensson, L. A.; Liljas, A. *J. Mol. Biol.* **1992**, *227*, 1192.
(45) Dennington, R., II; Keith, T.; Millam, J.; Eppinnett, K.; Hovell, W. L.; Gilliland, R. *GaussView*, Version 3.09; Semichem, Inc.: Shawnee Mission, KS, 2003.
(46) Siegbahn, P. E. M.; Borowski, T. *Acc. Chem. Res.* **2006**, *39*, 729–738.
(47) Frisch, M. J.; Trucks, G. W.; Schlegel, H. B.; Scuseria, G. E.; Robb, M. A.; Cheeseman, J. R.; Montgomery, J. A., Jr.; Vreven, T.; Kudin, K. N.; Burant, J. C.; Millam, J. M.; Iyengar, S. S.; Tomasi, J.; Barone, V.; Mennucci, B.; Cossi, M.; Scalmani, G.; Rega, N.; Petersson, G. A.; Nakatsuji, H.; Hada, M.; Ehara, M.; Toyota, K.; Fukuda, R.; Hasegawa, J.; Ishida, M.; Nakajima, T.; Honda, Y.; Kitao, O.; Nakai, H.; Klene, M.; Li, X.; Knox, J. E.; Hratchian, H. P.; Cross, J. B.; Bakken, V.; Adamo, C.; Jaramillo, J.; Gomperts, R.; Stratmann, R. E.; Yazyev, O.; Austin, A. J.; Cammi, R.; Pomelli, C.; Ochterski, J. W.; Ayala, P. Y.; Morokuma, K.; Voth, G. A.; Salvador, P.; Dannenberg, J. J.; Zakrzewski, V. G.; Dapprich, S.; Daniels, A. D.; Strain, M. C.; Farkas, O.; Malick, D. K.; Rabuck, A. D.; Raghavachari, K.; Foresman, J. B.; Ortiz, J. V.; Cui, Q.; Baboul, A. G.; Clifford, S.; Cioslowski, J.; Stefanov, B. B.; Liu, G.; Liashenko, A.; Piskorz, P.; Komaromi, I.; Martin, R. L.; Fox, D. J.; Keith, T.; Al-Laham, M. A.; Peng, C. Y.; Nanayakkara, A.; Challacombe, M.; Gill, P. M. W.; Johnson, B.; Chen, W.; Wong, M. W.; Gonzalez, C.; Pople, J. A. *Gaussian 03*, Revision E. 01; Gaussian, Inc.: Wallingford, CT, 2004.
(48) Mikulski, R. L.; Silverman, D. N. *Biochim. Biophys. Acta* **2010**, *1804* (20), 422–426.
(49) Chen, H.; Li, S.; Jiang, Y. *J. Phys. Chem. A* **2003**, *107* (23), 4652–4660.

JP101515H